Journal of Proteomics 152 (2017) 48–57

Contents lists available at ScienceDirect

Journal of Proteomics

journal homepage: www.elsevier.com/locate/jprot

Original Article

Specific adjustments in grapevine leaf proteome discriminating resistant and susceptible grapevine genotypes to *Plasmopara viticola*

Andreia Figueiredo [a,*], Joana Martins [b], Mónica Sebastiana [a], Ana Guerreiro [a], Anabela Silva [a], Ana Rita Matos [a], Filipa Monteiro [a], Maria Salomé Pais [a], Peter Roepstorff [c], Ana Varela Coelho [b]

[a] Biosystems & Integrative Sciences Institute (BioISI), Faculdade de Ciências da Universidade de Lisboa, 1749-016 Lisboa, Portugal
[b] Instituto de Tecnologia Química e Biológica, Universidade Nova de Lisboa, Av. da Republica, Oeiras 2780-157, Portugal
[c] Department of Biochemistry and Molecular Biology, University of Southern Denmark, Odense M, Denmark

ARTICLE INFO

Article history:
Received 13 July 2016
Received in revised form 22 October 2016
Accepted 24 October 2016
Available online 27 October 2016

Keywords:
Jasmonic acid
Lipid signalling
Protein modulation
Redox balance
Vitis vinifera

ABSTRACT

Grapevine downy mildew is an important disease affecting crop production leading to severe yield losses. This study aims to identify the grapevine cultivar-specific adjustments of leaf proteome that allow the discrimination between resistance and susceptibility towards *P. viticola* (constitutive (0 h) and in after inoculation (6, 12 and 24 h). Leaf proteome analysis was performed using 2D difference gel electrophoresis followed by protein identification via mass spectrometry. In addition, we analysed ROS production, antioxidant capacity, lipid peroxidation and gene expression. Proteins related to photosynthesis and metabolism allowed the discrimination of resistant and susceptible grapevine cultivars prior to *P. viticola* inoculation. Following inoculation increase of hydrogen peroxide levels, cellular redox regulation, establishment of ROS signalling and plant cell death seem to be key points differentiating the resistant genotype. Lipid associated signalling events, particularly related to jasmonates appear also to play a major role in the establishment of resistance. The findings from this study contribute to a better understanding of genotype-specific differences that account for a successful establishment of a defence response to the downy mildew pathogen.

Biological significance: Here, we present for the first time grapevine cultivar-specific adjustments of leaf proteome that allow the discrimination between resistance and susceptibility towards *P. viticola* (constitutive (0 h) and in after inoculation (6, 12 and 24 h). We have highlighted that, following inoculation, the major factors differentiating the resistant from the susceptible grapevine cultivars are the establishment of effective ROS signalling together with lipid-associated signalling events, particularly related to jasmonates. It is believed that plants infected with biotrophic pathogens suppress JA-mediated responses, however recent evidences shown that jasmonic acid signalling pathway in grapevine resistance against *Plasmopara viticola*. Our results corroborate those evidences and highlight the importance of lipid- signalling for an effective resistance response against the downy mildew pathogen.

1. Introduction

Grapevine downy mildew was introduced into European vineyards in the 1870s [1] and quickly spread to all major grape-producing regions of the world [2,3]. *Plasmopara viticola* (Berk. & Curt.) Berl. & de Toni, an obligate biotrophic oomycete, is the causal agent of this devastating disease. While American and Asiatic Vitis species present genetic resistance to this pathogen, domesticated grapevine *Vitis vinifera* is sensitive to downy mildew. As a control measure, several fungicide applications are necessary every year and *P. viticola* resistance has already been found to the most common fungicides [4,5]. Only in the past few decades, resistance breeding partly replaced the chemical plant protection applied against grapevine downy mildew. Partially resistant grapevine varieties resulted from breeding programs by introgression of resistant traits from wild *Vitis* spp. (eg *V. labrusca, V. amurensis*). However, recent reports have shown that *P. viticola* presents a high evolutionary potential as several isolates were able to develop fungicide resistance [4,5] and to break down plant resistance of interspecific hybrids [6,7]. These findings have highlighted the need for a better understanding of grapevine resistance mechanisms against *P. viticola*.

Several studies have reported that aside from constitutive physical and chemical barriers, downy mildew resistance is mainly based on post-infection processes [8,9]. The susceptibility of *Vitis vinifera* to downy mildew suggests that this species lacks a *P. viticola*-specific recognition system [10]. However, transcriptional [8,11–14] and proteomic [15] changes associated with the early stages of *P. viticola* infection indicate the presence of a weak, but insufficient, defence response in

* Corresponding author.
E-mail address: aafigueiredo@fc.ul.pt (A. Figueiredo).

http://dx.doi.org/10.1016/j.jprot.2016.10.012
1874-3919/

susceptible grapevines. In our previous studies we have characterized the cultivar-specific responses to *P. viticola* inoculation by direct comparison of a resistant (Regent) and a susceptible (Trincadeira) cultivar prior and post inoculation with the downy mildew pathogen [14,16,17]. These studies have clearly shown that there is a remodelling of transcripts associated to defence and signalling in the resistant genotype [14] and that at the metabolome level, Regent presents higher levels of phenolic compounds and stress-related metabolites that increase as soon as 6 hpi [17].

Grapevine proteomic data are scarce [18]. The proteome modulation during the infection process is poorly characterized and only few studies have been published so far in compatible interactions [15,19]. We have used a differential gel electrophoresis (DIGE) approach to identify the key differences in proteome modulation of two *Vitis vinifera* genotypes, Regent (resistant) and Trincadeira (susceptible) prior (0 h) and at 6, 12 and 24 h post inoculation (hpi) with *P. viticola*. Gene expression and biochemical analysis on hydrogen peroxide content, total antioxidant capacity and lipid peroxidation were also conducted. This study characterizes for the first time the grapevine genotype-specific proteome alterations that account for resistance against *P. viticola*, highlighting the importance of the early activation of ROS and lipid associated signalling for the establishment of the incompatible interaction.

2. Material and methods

2.1. Plant material, inoculum and pathogen infection

Plants from *V. vinifera* cultivars Regent and Trincadeira were propagated under identical greenhouse conditions as described by [14]. *Plasmopara viticola* inoculum was collected after an overnight incubation of symptomatic leaves from greenhouse infected plants in a moist chamber at room temperature. Sporangia were carefully recovered by brushing, dried, stored at −25 °C. Vitality was checked by microscopy [20]. A suspension containing 10^4 sporangia mL^{-1} was used to spray the abaxial leaf surface in order to challenge the plants. Inoculated plants were incubated overnight in the dark at 25 °C and 99–100% relative humidity and then kept under controlled greenhouse conditions during inoculation time-course. For each biological replicate two leaves (third to fifth from the shoot apex) from three different plants were harvested at 0 h, 6, 12 and 24 hpi, immediately frozen in liquid nitrogen and stored at −80 °C. Four independent biological replicates were collected. An experimental design scheme is presented in Supplementary Fig. 1.

2.2. Protein sample preparation

Protein extraction was done using a phenol based protocol according to [21], four biological replicates were extracted from each condition. Protein concentration was determined with a 2-D Quant Kit (GE Healthcare) using BSA (2 mg/mL) as standard. Extraction yield for our samples was around 2.95 ± 0.33 mg per gram of fresh weight. Further purification was done with the Ettan 2D Clean-up kit (GE Healthcare) according to manufacturer's recommendations. The recovered precipitated protein was solubilized in 30 μL of labeling buffer and pH was adjusted to 8.5 using NaOH (100 mM).

2.3. Experimental design and CyDye protein labeling

Each sample was covalently labeled with fluorescent dyes, either Cy3 or Cy5 (400 pmol of dye per 50 μg of protein) and a dye swap between both fluophores was used to avoid problems associated with preferential labeling. Sample pairs run in each gel were randomized in order to avoid bias of the experimental results. A mixture of equal amounts of protein from every sample in the experiment was labeled with Cy2 and used as internal standard. Dye labeling scheme is presented (Supplementary Fig. 1).

2.4. 2D gel electrophoresis

The labeled samples were combined (Cy3, Cy5 and Cy2), to a final of 150 μg protein and mixed with 150 μL of 8 M urea, 4% (*w*/*v*) CHAPS, 130 mM DTE, 2% (*v*/v) and pharmalytes pH 4–6.5, adjusted to a final volume of 450 μL with rehydratation buffer (8 M urea, 4% (*w*/*v*) CHAPS, 13 mM DTE, 1% (*v*/v) pharmalytes pH 4–6.5) and submitted to isoelectric focusing (IEF) as the first-dimension separation.

IPG strips, pH 4–7 IPG-strips (24 cm, linear gradient; GE Healthcare) were actively rehydrated overnight for 18 h at 50 V. IEF was performed in a IPGphor3 system from GE Healthcare at 20 °C (100 V for 2 h; 3 h 500 V, 4 h 1000 V, 1 h gradient from 1000 V to 3500 V, 3 h 3500 V, 4 h gradient from 3500 V to 8000 V, until 98 kVh). After the IEF, IPG strips were equilibrated for 15 min in equilibration buffer (6 M Urea, 2% (*w*/*v*) SDS, 50 mM Tris pH 8.8, 0.02% (*w*/*v*) bromophenol blue, 30% (*v*/v) glycerol) supplemented with 2% (*w*/*v*) DTE, followed by alkylation for 15 min in equilibration buffer supplemented with 3% (*w*/*v*) iodocetamide.

SDS-PAGE was carried out as the second-dimension separation in 12.5% polyacrilamide resolving gels in an Ettan DALT twelve system (GE Healthcare). The separation was run at 20 °C overnight with 1st step at 80 V, 10 mA/gel and 1 W/gel, 2nd step at 100 V, 17 mA/gel and 1.5 W/gel.

2.5. Scanning and image analysis

2D–DIGE gels were scanned at a pixel size of 100 μm using a Laser-based scanner FLA-5100 (FujiFilm) and Image Reader FLA 500 version 1.0 (FujiFilm) at three different wavelengths characteristic of the different CyDyes. Gel images were exported into Progenesis SameSpot V4.5 image analysis system (Nonlinear Dynamics, Newcastle, UK), where quantitative analysis of protein spots was performed. Automatic and subsequent manual editing, aligning, spot volume normalization and matching procedures were done as part of the Progenesis SameSpot workflow. Variation of protein expression was considered statistically significant if the absolute abundance variation was at least 1.5-fold between spots of any experimental group with a *p-value* ≤ 0.05 by ANOVA anda power value ≥ 0.7 (Progenesis SameSpot V4.5, Nonlinear Dynamics, Newcastle, UK). Unsupervised PCA correlation analysis was performed using the statistical tool withinSIMCA V13.0.3.0 (Umetrics) (Supplementary Table 1, Fig. 1). The spots of interest were visually checked and selected for protein identification by mass spectrometry.

2.6. Protein identification by mass spectrometry

Differentially accumulated protein spots were excised from the preparative 2-DE gels loaded with 600 μg of protein and stained with colloidal CBB [22]. Proteins were trypsin-digested, peptides were acidified with formic acid, desalted, concentrated with POROS R2 microcolumns (Applied Biosystems, Foster City, CA) and co-crystallised onto MALDI sample plates using the matrix α-cyano-4-hydroxycinnamic acid as described previously [23]. MS and MS/MS spectra were acquired using a MALDI-TOF/TOF 4800 plus MS/MS (Applied Biosystems, Foster City, CA, USA). The equipment was externally calibrated using des-Arg-Bradykinin (904.468 Da), angiotensin 1 (1296.685 Da), Glu-Fibrinopeptide B (1570.677 Da), ACTH (1–17) (2093.087 Da), and ACTH (18–39) (2465.199 Da) (4700 Calibration Mix, Applied Biosystems, Foster City, CA, USA). Each reflectron MS spectrum was collected in a result-independent acquisition mode, typically using 1000 laser shots per spectra and a fixed laser intensity of 3500 V. The 15 strongest precursors were selected for MS/MS, the weakest precursors being fragmented first. MS/MS analyses were performed using CID (Collision Induced Dissociation), with collision energy of 1 kV and a gas pressure of 1×10^{-6} Torr. Two thousand laser shots were collected for each MS/MS spectrum using a fixed laser intensity of 4500 V.

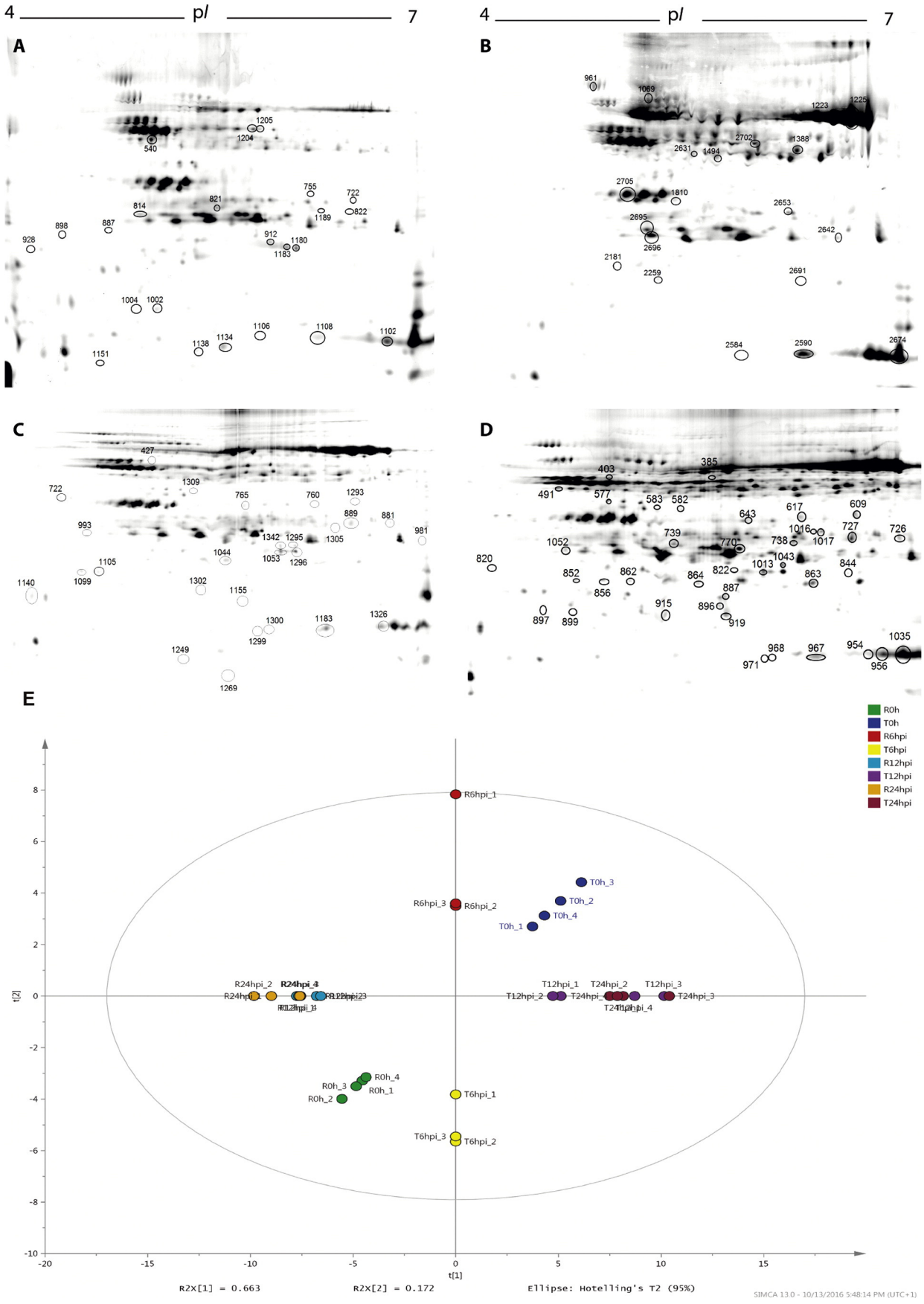

Fig. 1. Representative two-dimensional gel electrophoresis map when comparing *V. vinifera* cv Regent and Trincadeira leaf proteome prior (A-0 h) and after (B-6 hpi; C-12 hpi; D-24 hpi) inoculation with *Plasmopara viticola*. Differentially accumulated spots for each time-point are represented. Protein identifications are presented in Supplementary Table 3. Principal component analysis (E) of the differential protein profiles in Regent and Trincadeira at 0 h, 6, 12 and 24 hpi with *Plasmopara viticola*. The plot shows principal component 1 (PC1) on X axis and principal component 2 (PC2) on Y axis, together they explain 84% of the selected spots variability. Colored dots represent the different gels.

The MS and MS/MS spectra were searched against the NCBI protein database restricted to *Vitis* (156,682 entries), and the predicted Pinot Noir grapevine proteome (http://genomes.cribi.unipd.it/grape/ [24]) using MASCOT (v. 2.2; Matrix Science, Boston, MA, USA) embedded into GPS-Explorer Software 3.6 (Applied Biosystems) with the following parameter settings: trypsin cleavage; one missed cleavage allowed; carbamidomethylation as fixed modification; oxidation of methionines as variable modification; minimum mass accuracy of 30 ppm for the parent ions and fragment tolerance of ± 0.3 Da. All searches were evaluated based on the significant scores obtained from MASCOT (≥ 70). Both protein score and total ion score confidence intervals percentage were set above 95%, and a $p < 0.05$ was set as the significance threshold for MS/MS. Proteins identified as "unnamed" were queried against the NCBI nr database (Blast p; E value < e^{-35}). The mass spectrometry proteomics data have been deposited to the ProteomeXchange Consortium [25] via the PRIDE partner repository with the dataset identifier PXD002920.

2.7. Bioinformatics analysis

Each protein was classified according to the biological process and molecular function using GO (Gene Ontology) annotation [26]. Subcellular locations of the unique proteins identified in this study were predicted using the publicly available programs Mempype [http://mu2py.biocomp.unibo.it/mempype/default/index] and PlantLoc ([http://cal.tongji.edu.cn/PlantLoc/index.jsp].

2.8. Determination of H_2O_2 content

Hundred mg of plant material were homogenized in a phosphate buffered saline solution (PBS) with 1–4% (*w*/*v*) of insoluble polyvinylpolypyrrolidone ($PVPP_{40000}$). Samples were centrifuged at 16,000 × *g* for 1 min, the supernatant was collected and used for the assay. Concentration of hydrogen peroxide was measured spectrophotometrically at 405 nm following the method described by [27] based on the oxidation the chromogen 2′,2-azino-di(3-ethylbenzathiazoline-6-sulphonic acid) (ABTS) catalyzed by a peroxidase in the presence of H_2O_2. A standard curve with known concentrations of H_2O_2 was used and data was expressed as micromoles per gram of fresh weight. Three biological replicates and two technical replicates were used.

2.9. Antioxidant capacity assay

Leaf extracts were done as described for the H_2O_2 assay. Total antioxidant capacity was measured spectrophotometrically at 405 nm using the antioxidant assay kit (Sigma-Aldrich) according to manufacturer's instructions. A standard curve with known concentrations of Trolox was used and data were normalized by protein content. Three biological replicates and two technical replicates were used.

2.10. Lipid peroxidation

Lipid peroxidation was measured following the thiobarbituric acid (TBA) reacting substance (TBARS) protocol [28]. Hundred mg of frozen tissue were homogenized in ethanol 80% (*v*/v) and centrifuged at 14,000 × *g* for 5 min at 4 °C. The supernatants reacted with TBA solution at 95 °C for 30 min. Absorbance at 440, 532 and 600 nm was determined after a 10 min centrifugation at 14,000 × *g*, 4 °C. Malonaldehyde (MDA) equivalents (nmol mL^{-1}) = [(A − B) × 106] / 157,000, where A = [[(Abs532 + TBA) − (Abs 600 + TBA)] − [(Abs 532 − TBA) − (Abs 600 − TBA)]] and B = [[(Abs 440 + TBA) − (Abs 600 + TBA)] × 0.0571].

2.11. Expression analysis

Total RNA extraction and cDNA synthesis were done according to Ref. [21]. Four genes associated with Jasmonic Acid (JA) biosynthesis and 1 gene associated with lipid signalling were selected for analysis. Quantitative RT-PCR (qPCR) experiments were carried out using Maxima™ SYBR Green qPCR Master Mix (2×) kit (Fermentas, Ontario, Canada) in a StepOne™Real-Time PCR system (Applied Biosystems, Sourceforge, USA) as described in Ref. [21]. Data was normalized according to Ref. [21]. Gene specific primers, amplicon length, annealing and melting temperatures and amplification efficiencies are described in Supplementary Table 2. Gene expression (fold change) was calculated according to [29].

2.12. Statistical analysis

Statistical significance ($p \leq 0.05$) between the two genotypes was determined for ROS production, antioxidant capacity, lipid peroxidation and gene expression by the Mann-Whitney *U* test using IBM SPSS Statistics version 21.0 (SPSS Inc., USA) software.

3. Results and discussion

The proteome differences of two *Vitis vinifera* cultivars, Regent and Trincadeira (resistant and susceptible to downy mildew, respectively) were analysed prior (0 h) and after *P. viticola* inoculation (6, 12 and 24 hpi) by 2D–DIGE followed by MS-based protein identification. By direct comparison of both grapevine genotypes (Regent was labeled as the test sample and Trincadeira as control), we were able to identify the proteins that discriminated both genotypes either constitutively or in response to the pathogen.

3.1. 2D–DIGE and differential expression analysis

2D–DIGE gel reference maps resolved a total of 758 spots at 0 h; 975 at 6 hpi; 874 at 12 hpi and 695 at 24 hpi. Two-way ANOVA discriminated 122 protein spots with abundance changes across all the compared time-points, for subsequent protein identification (fold-change > 1.5, ANOVA $p < 0.05$, Supplementary Table 1). A clear distinction in proteome between the two grapevine genotypes was also confirmed by PCA (Fig. 1E). This unsupervised PCA bi-plot, explains 66.3% (PC1) and 17.2% (PC2) and shows a gel grouping (colored dots) which agrees with the experimental groups. The two grapevine genotypes are separated although the gels of 12 and 24 hpi, for each genotype, plot quite closely, indicating that the differences between them are minimal in relation to the 0 h and 6 hpi changes. At 0 h, 24 spots (19.6%) discriminated both grapevine genotypes. After inoculation with *P. viticola*, 23 spots (18.9%) were differentially accumulated at 6 hpi, 28 (23%) spots at 12 hpi and 47 spots (38.5%) at 24 hpi. An increased number of infection responsive proteins when comparing both genotypes at 24 hpi suggest that although larger transcriptional changes occur as soon as 6 hpi, in response to the pathogen inoculation [14], a larger genotype-dependent proteomic change occurs at 24 hpi. Representative maps for the grapevine leaf resolved proteome at 0 h, 6, 12 and 24 hpi on which the differentially accumulated spots are outlined is presented in Fig. 1(A-D).

3.2. Protein identification and annotation

Of the 122 differentially accumulated protein spots, 99 were successfully annotated (Supplementary Table 3) accounting for 50 unique proteins (Table 1, Supplementary Table 4). The majority of the proteins were only accumulated in one of the time-points analysed, 12 proteins showed a differential pattern of accumulation in two time-points, 6 proteins were simultaneously accumulated in three time-points and only one protein was differentially accumulated prior and after *P. viticola*

Table 1
Identification, regulation and functional categorization of the differentially acumulated proteins when comparing the two *Vitis vinifera* cultivars Regent (resistant) and Trincadeira (susceptible) prior (0 h) and after (6, 12 and 24 h) inoculation with *P. viticola*.

Time-course with fold change (VR/VT)[a]										Matched peptide[c]		
0 h	6 hpi	12 hpi	24 hpi	Protein identification	NCBI Acc. number	Theoretical MW (Da)	Theoretical pI	Anova *p* value	Mascot score[b]	SC (%)[d]	MS	MSMS
Photosynthesis and carbohydrate metabolism												
2.22		3.1	2.61	PREDICTED: ribulose bisphosphate carboxylase small chain, chloroplastic [*Vitis vinifera*]	XP_003634190.1	21,267.58	9.11	0.000	295	71	14	2
2.17	2.51	1.99	2.26	ribulose-1,5-bisphophate carboxylase/oxygenase small subunit [Vitis pseudoreticulata]	ABC86738.1	20,456.51	9.06	0.015	201	33	6	1
−2.22				ribulose-1,5-bisphophate carboxylase/oxygenase small subunit [Vitis pseudoreticulata]	ABC86738.1	20,456.51	9.06	0.001	203	21	5	1
	1.85	−1.62	−2.92	ribulose-1,5-bisphosphate carboxylase/oxygenase large subunit [Vitis vinifera]	YP_567084.1	52,518.78	6.33	0.008	1080	56	20	9
		2.25	2.96	PREDICTED: ribulose bisphosphate carboxylase/oxygenase activase 1, chloroplastic-like [Vitis vinifera]	XP_002270571.2	51,880.97	5.69	0.024	803	51	17	6
−1.58	1.88		−3.70	PREDICTED: oxygen-evolving enhancer protein 2, chloroplastic [Vitis vinifera]	XP_002283048.1	27,794.15	8.33	0.007	180	50	8	2
	1.90			PREDICTED: chlorophyll *a*-b binding protein 8, chloroplastic [Vitis vinifera]	XP_002273201.1	29,529.81	7.84	0.012	116	20	6	3
−4.23		−1.53		PREDICTED: cytochrome *b*6-f complex iron-sulfur subunit, chloroplastic isoform 1 [Vitis vinifera]	XP_002284361.1	24,075.74	8.52	0.000	120	44	5	1
		−1.53		PREDICTED: cytochrome *b*6-f complex iron-sulfur subunit, chloroplastic-like [Vitis vinifera]	XP_002265183.2	22,519.99	8.26	0.023	82	6	1	1
	−1.64			PREDICTED: thylakoid lumenal 29 kDa protein, chloroplastic-like isoform X1 [*Citrus sinensis*]	XP_010664348.1	37,487.45	6.65	0.006	275	54	16	2
			−12.33	PREDICTED: thylakoid lumenal 19 kDa protein, chloroplastic-like [Vitis vinifera]	XP_002275752.1	26,702.96	6.91	0.000	447	54	10	5
		2.97		PREDICTED: photosystem II stability/assembly factor HCF136, chloroplastic [Vitis vinifera]	XP_002278958.1	44,272.10	6.92	0.000	1600	64	22	11
				PREDICTED: cysteine synthase [Vitis vinifera]	XP_003633658.1	34,369.87	5.39	0.000	104	3.7	7	1
−1.56		−1.94	−2.68	PREDICTED: carbonic anhydrase 1 [*Arabidopsis thaliana*]	XP_002277957.1	36,544.96	8.06	0.000	454	18	5	2
		−6.92		PREDICTED: triosephosphate isomerase, chloroplastic-like isoform 1 [Vitis vinifera]	XP_002274871.1	34,675.35	8.13	0.001	546	39	9	5
		−2.93		PREDICTED: triosephosphate isomerase, cytosolic [Vitis vinifera]	XP_002283693.1	27,128.22	6.35	0.000	949	86	18	8
−1.88			1.55	PREDICTED: sedoheptulose-1,7-bisphosphatase, chloroplastic [Vitis vinifera]	XP_002263049.1	42,525.37	5.95	0.006	364	20	8	4
1.72				PREDICTED: phosphoglycerate kinase, chloroplastic isoform 1 [Vitis vinifera]	XP_002263796.1	50,083.05	8.26	0.012	147	19	5	1
3.40	1.44			PREDICTED: probable fructose-bisphosphate aldolase 2, chloroplastic-like [Vitis vinifera]	XP_003631873.1	42,803.96	7.55	0.001	869	55	15	6
			−2.36	PREDICTED: probable fructose-bisphosphate aldolase 1, chloroplastic [Vitis vinifera]	XP_002267726.1	42,948.22	8.13	0.000	300	19	2	2
	−1.66			PREDICTED: glyceraldehyde-3-phosphate dehydrogenase B, chloroplastic isoform 1 [Vitis vinifera]	XP_002273754.1	48,120.05	7.60	0.012	256	32	14	2
Respiration												
−1.40				PREDICTED: gamma carbonic anhydrase 1, mitochondrial-like [*Cucumis sativus*]	XP_002282021.1	29,442.61	5.89	0.017	772	56	11	7
General metabolism												
		1.37		PREDICTED: glycine cleavage system H protein, mitochondrial isoform 1 [Vitis vinifera]	XP_002280707.1	17,553.62	5.07	0.007	92	33	2	0
4.32				PREDICTED: cysteine synthase [Vitis vinifera]	XP_003633658.1	34,369.87	5.39	0.002	140	41	8	1
1.48				PREDICTED: glutamine synthetase leaf isozyme, chloroplastic [Vitis vinifera]	XP_002279497.1	47,914.26	7.58	0.007	407	47	14	3
Energy												
	1.71			PREDICTED: ATP synthase gamma chain, chloroplastic-like isoform 1 [Vitis vinifera]	XP_002275015.1	41,018.23	5.95	0.012	74	14	4	1
				Predicted: quinone oxidoreductase-like protein At1g23740, chloroplastic-like [Vitis vinifera]	XP_003631255.1	40,071.98	8.61	0.012	69	4.8	2	1
			1.39	PREDICTED: ATP synthase delta chain, chloroplastic [Vitis vinifera]	XP_002274963.1	26,385.31	8.85	0.004	274	27	6	4
Redox homeostasis												
1.52			1.54	type II peroxiredoxin E [Vitis vinifera]	NP_001268192.1	22,511.02	7.67	0.001	671	56	11	6
			−1.50	type II peroxiredoxin F [Vitis vinifera]	NP_001268077.1	21,825.08	8.74	0.022	68	9	2	1
		1.50	−1.70	PREDICTED: thioredoxin-like protein CDSP32, chloroplastic [Vitis vinifera]	XP_002285902.1	33,454.35	6.38	0.004	1090	49	16	10
−1.56		−1.44		manganese superoxide dismutase [Vitis vinifera]	XP_010658132.1	25,283.90	6.80	0.001	377	25	10	4
		−1.63	−1.51	PREDICTED: L-ascorbate peroxidase 2, cytosolic [Vitis vinifera]	XP_002284767.1	27,557.42	5.71	0.000	888	39	13	7
			−1.91	PREDICTED: ferredoxin-thioredoxin reductase,	XP_002271306.1	18,122.48	8.97	0.001	170	23	4	1

Table 1 (*continued*)

Time-course with fold change (VR/VT)[a]										Matched peptide[c]		
0 h	6 hpi	12 hpi	24 hpi	Protein identification	NCBI Acc. number	Theoretical MW (Da)	Theoretical pI	Anova *p* value	Mascot score[b]	SC (%)[d]	MS	MSMS
				variable chain, chloroplastic [Vitis vinifera]								
Defence												
−4.32		−5.77	1.51	abscisic stress ripening protein [Vitis pseudoreticulata]	ABC86744.1	16,688.98	5.68	0.000	1050	57	10	6
			−3.23	abscisic stress ripening protein [Vitis pseudoreticulata]	ABC86744.1	16,688.98	5.68	0.000	898	42	7	5
	1.78		1.45	PREDICTED: MLP-like protein 423 [Vitis vinifera]	XP_002267219.1	27,397.35	7.99	0.010	346	43	6	3
	−1.55	−1.86	−2.51	PREDICTED: peptidyl-prolyl cis-trans isomerase CYP20–3, chloroplastic-like isoform 1 [Vitis vinifera]	XP_002273421.2	27,397.35	7.99	0.010	431	41	11	4
	−1.64			pathogenesis-related protein 10 [Vitis pseudoreticulata]	AEG64701.1	17,128.57	5.96	0.003	367	65	8	3
		1.85		putative plastid lipid-associated protein [Vitis hybrid cultivar]	BAF95867.1	25,890.45	4.85	0.011	95	10	2	1
			2.91	Tetratricopeptide repeat 30A [*Gossypium arboreum*]	KHG00819.1	36,824.58	6.30	0.000	156	19	4	1
	1.77			PREDICTED: heat shock cognate 70 kDa protein isoform 2 [Vitis vinifera]	XP_002283532.2	71,170.50	5.16	0.005	75	6	3	0
−1.50			−1.72	PREDICTED: glycine-rich RNA-binding protein GRP1A-like [Vitis vinifera]	XP_003631658.1	16,329.28	6.32	0.009	375	47	6	3
		2.33	−1.42	PREDICTED: 29 kDa ribonucleoprotein A, chloroplastic [Vitis vinifera]	XP_002281642.1	31,510.99	5.21	0.020	187	28	6	1
			−1.5	PREDICTED: 28 kDa ribonucleoprotein, chloroplastic [Vitis vinifera]	XP_002278832.1	36,394.30	4.60	0.001	96	4	6	1
			−6.03	PREDICTED: 18.2 kDa class I heat shock protein isoform 2 [Vitis vinifera]	XP_003633470.1	17,021.28	5.80	0.000	250	17.8	5	2
			−1.45	PREDICTED: 18.1 kDa class I heat shock protein [Vitis vinifera]	XP_002280353.1	18,193.51	6.17	0.001	82	9	1	1
	4.11			PREDICTED: glyceraldehyde-3-phosphate dehydrogenase A, chloroplastic-like [Vitis vinifera]	XP_002278352.1	43,155.11	7.00	0.010	208	10	4	2
Protein metabolism												
			1.62	PREDICTED: elongation factor Tu, chloroplastic-like [Vitis vinifera]	XP_002277301.1	52,692.38	6.24	0.000	1150	57	23	9
		1.83		PREDICTED: 50S ribosomal protein L12, chloroplastic [Vitis vinifera]	XP_002277258.1	19,662.75	5.82	0.017	723	42	10	6
	−1.54			PREDICTED: 20 kDa chaperonin, chloroplastic [Vitis vinifera]	XP_002277861.1	26,321.37	9.37	0.023	710	60	12	4
	−1.65			PREDICTED: nascent polypeptide-associated complex subunit alpha-like [Vitis vinifera]	XP_002266597.1	22,027.32	4.34	0.026	324	44%	6	3
			−8.78	PREDICTED: proteasome subunit beta type-2-A-like [Vitis vinifera]	XP_003632316.1	22,490.68	5.85	0.000	333	25%	4	3
Unknown												
1.57			1.90	PREDICTED: uncharacterized protein LOC100259089 [Vitis vinifera]	XP_002266585.1	21,746.28	4.96	0.007	110	41%	5	1

When the same protein identification was obtained for several spots, data for the spot presenting higher protein score is presented.

[a] Fold change (VR/VT): increment/decrease of the spot intensities in resistant (VR)/control (VT) conditions. Negative fold means that the protein was less abundant in resistance conditions. Positive fold change means that proteins were more abundant in resistance conditions.

[b] Mascot Score: MS and MSMS scores are based on the calculation probability that the observed match between the experimental data and the database sequence is a random event. Minimum score considered - 70.

[c] Matched peptide: refers the number of peptide of the protein sequence that corresponds to matched peptides.

[d] SC % (Sequence covered): refers the percentage of the peaks intensity that correspond to matched peptides.

inoculation (Supplementary Fig. 2a). Two proteins presented an altered accumulation pattern at all time points after inoculation (6, 12 and 24 hpi): peptidyl-prolyl cis-trans isomerase cyp 20-3 and ribulose-1,5-bisphosphate carboxylase/oxygenase large subunit.

Gene ontology (GO) annotation and the physiological functions allowed the classification of the identified proteins into 8 categories (Supplementary Fig. 2b): photosynthesis and carbohydrate metabolism (21), respiration (1), general metabolism (3), energy (2), redox homeostasis (6), defence (11), protein metabolism (5) and unknown function (1). At 6 hpi the number of differentially accumulated protein spots increased in the defence category and at 12 and 24 hpi the defence and redox homeostasis categories become two of the most represented. Within the defence category, the number of protein spots presenting GO terms associated to "stress response" increased during inoculation time-course in both genotypes and at 24 hpi categories such as "death", "single organism signalling" and "detection of stimulus" appeared only in the resistant genotype.

3.3. Proteome discrimination of grapevine genotypes (0 h)

The possibility to discriminate genotypes according to their proteome profile has already been demonstrated for walnut [30] and tomato [31]. When comparing the grapevine cultivars Regent and Trincadeira, prior to *P. viticola* inoculation, 24 protein spots allowed genotype differentiation and of those 19 were identified. Several spots that differentiated the resistant genotype were identified as proteins involved in photosynthesis, carbohydrate and general metabolism. Higher accumulation of proteins related with primary metabolism and biosynthetic machinery in Regent could pay for the fitness cost of the constitutive resistance, hence resulting in more stress-resistant plants.

3.3.1. Genotype-specific protein modulation upon P. viticola inoculation

Upon inoculation photosynthesis and carbohydrate- related proteins were down-acumulated in Regent from 12 hpi (Table 1) which is in accordance to other studies on the same pathosystem [15,19]. However, the high turnover of photosynthetic proteins such as the ribulose bisphosphate carboxylase/oxygenase activase 1, ribulose-1-5-bisphosphate carboxylase small subunit and the photosystem II stability/assembly factor HCF136 in the resistant grapevine genotype, suggests that Regent may be evoking defence mechanisms to protect the photosynthetic machinery recovering photosynthetic efficiency upon *P. viticola* inoculation. This was previously reported for other incompatible interactions [32,33].

3.3.2. Oxidative burst, ROS signalling and plant cell death

ROS play an important role in pathogen resistance by directly strengthening host cell walls via cross-linking of glycoproteins, lipid peroxidation and activation of ROS-signalling networks leading to the establishment of a resistance response [34]. Additional regulatory functions for ROS in defence occur in conjunction with other plant signalling molecules, particularly with salicylic acid (SA) and nitric oxide (NO) [34]. After inoculation with *P. viticola*, H_2O_2 accumulation occurred in both grapevine genotypes with the production of H_2O_2 being quicker and stronger in Regent (6 hpi: 2.14 ± 0.23 μmol H_2O_2 g^{-1} FW) while in Trincadeira only a slight increase was detected at 6 hpi and 12 hpi (6 hpi: 0.56 ± 0.09 μmol H_2O_2 g^{-1} FW; 12 hpi: 0.74 ± 0.09 μmol H_2O_2 g^{-1} FW; Fig. 2A). Indeed a transient oxidative burst and a subsequent temporary shift in the intracellular redox state are common features of both biotic and abiotic stress responses [35] and an higher accumulation of H_2O_2 in resistant genotypes sooner than in susceptible ones has been reported for many plant pathogen interactions [36,37]. Whether ROS will act as damaging or signalling molecule depends on the delicate equilibrium between ROS production and scavenging after pathogen inoculation, achieved by an efficient antioxidative system, comprising the non-enzymatic as well as enzymatic antioxidants [35], these systems may restrict the ROS-dependent damage or finely tune ROS-dependent signal transduction. After inoculation with *P. viticola*, and despite the ROS burst in the resistant genotype, the total antioxidant capacity did not differ significantly between the two cultivars (Fig. 2, B). In Regent, there was only a slight increase in the total antioxidant capacity during inoculation time-course (Fig. 2, B). In fact, in the resistant genotype, there was a decrease in the abundance of several proteins associated to ROS scavenging at 12 and 24 hpi (manganese superoxide dismutase (spot 1305), L-ascorbate peroxidise (spots 760, 1017), type II peroxiredoxin F (spot 844), thioredoxin-like protein CDSP32 (spot 617), and ferredoxin-thioredoxin reductase (Spot 896)) (Table 1, Supplementary Table 3). A key factor in incompatible interactions and cell death responses is the secondary production of ROS, either by positive feedback enhancement of the primary oxidative signal or by inactivation of antioxidative capacity [38]. By maintaining a low abundance of ROS scavenging proteins and not increasing the total antioxidant capacity, Regent may be promoting the secondary production of ROS following pathogen recognition as it has been previously described [39–42]. Moreover, a lower abundance of ROS scavenging proteins may be directly related to salicylic acid and nitric oxide contents [38,40]. Indeed, we have recently reported an increase in SA content from 6 hpi of *V. vinifera* cv Regent with *P. viticola* [43]. Greater availability of ROS has also been shown to lead to the increased glutathione content leading to the induction or activation of thioredoxins and glutaredoxins that are able to reduce the SA receptor NPR1that in turn interacts with TGA transcription factors to induce PR gene expression leading to the establishment of the hypersensitive response [44].

Two ROS-scavenging proteins presented higher abundance in the Regent at 12 and 24 hpi (thioredoxin-like protein (Trxs) CDSP32 and a type II peroxiredoxin E (PrxII E, respectively). Both Trx CDSP32 and PrxII E are chloroplastic and Trx CDSP32 functions as an electron donor to Prx. The balance between ROS and peroxinitrite determines PrxII E activity, which in turn may modulate the cell death program and protein tyrosine nitration during hypersensitive response [45,46]. Moreover, a heat shock cognate 70 (HSC70) chaperone (spot 1069) presented higher abundance in Regent at 6 hpi. This protein has been shown to regulate *Arabidopsis* immune responses [47] and to be involved in both positive and negative regulation of cell death and immunity signalling [48,49]. GAPDHa (spot 2590), recently associated to cellular redox regulation, ROS signalling and apoptosis [50] also presented higher abundance in Regent at 6 hpi and previously, it has been reported in the same pathosystem an increase of expression of the IQ calmodulin binding region-apoptosis regulator Bcl-2 protein (BAG, HS07576) at 6 hpi of *V. vinifera* cv Regent with *P. viticola* [14]. Our data suggests that ROS production, ROS associated signalling and

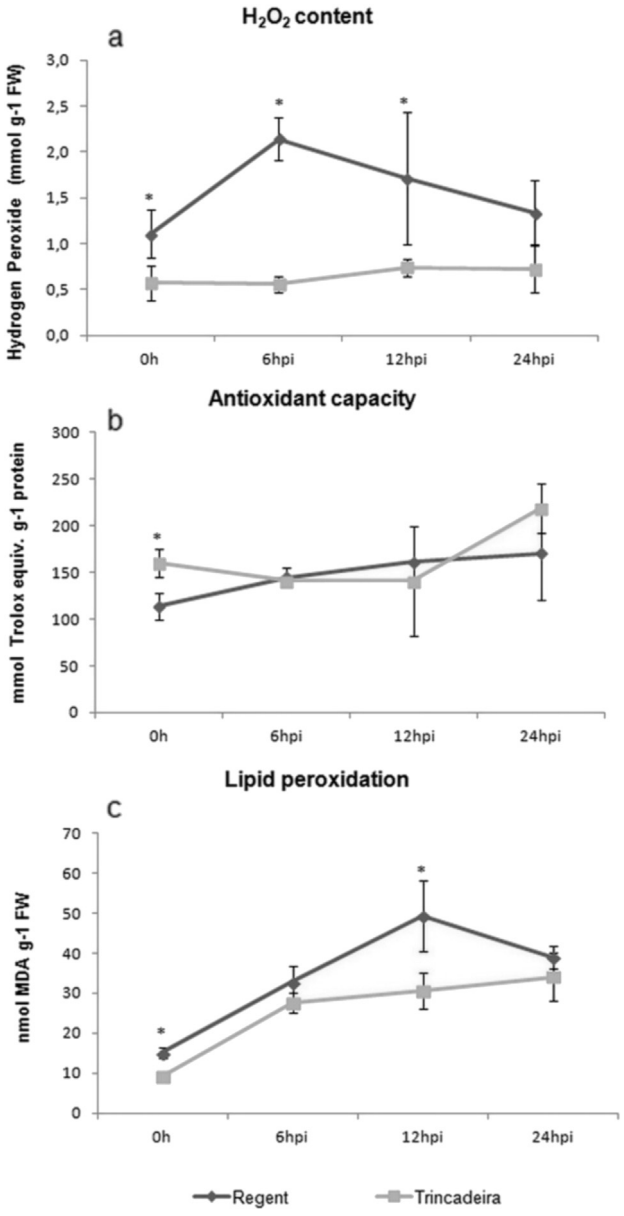

Fig. 2. ROS production, antioxidant capacity and lipid peroxidation in grapevine leaves of Regent and Trincadeira at 0 h, 6, 12 and 24 hpi with *P. viticola*: (a) Hydrogen peroxide generation (μmol Hydrogen peroxide g^{-1} FW); (b) total antioxidant capacity (μmol Trolox equiv. mg^{-1} protein); (c) MDA content (nmol MDA equiv. g^{-1} FW). Mean and standard deviation of three biological replicates is presented. * represents statistically significant differences between the two grapevine genotypes ($P \leq 0.05$; Mann-Whitney *U* test).

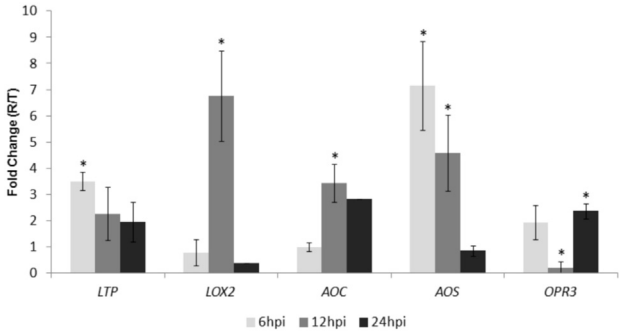

Fig. 3. qPCR expression profiling of *LOX2*, *AOS*, *AOC*,*OPR3* (associated to JA biosynthesis) and *LTP1* (lipid signalling). Mean and standard deviation of four biological replicates is presented. Fold change reveals the comparison of gene expression between Regent and Trincadeira inoculated samples at 6, 12 and 24 h post inoculation with *P. viticola*. * represents statistically significant differences between the two grapevine genotypes ($P \leq 0.05$; Mann-Whitney *U* test).

the establishment of a hypersensitive response are distinctive feature differentiating the resistant cultivar Regent, from the susceptible cultivar Trincadeira.

3.3.3. Lipid associated signalling

One of the key processes in early plant defence signalling is enhanced lipid peroxidation and production of a vast array of oxylipins. Despite lipid peroxidation being often linked to cell apoptosis, necrosis and programmed cell death it is also linked to the synthesis of jasmonic acid [51]. Moreover, lipid peroxidation products, such as MDA or 4-HNE, have been described as signalling molecules in regulation of several transcription factors sensible to stress [52]. After inoculation with *P. viticola*, lipid peroxidation increased in both Regent and Trincadeira (Fig. 2C), but MDA content at 12 hpi was much higher in the resistant genotype (Regent: 49.26 ± 8.94 nmol MDA g^{-1} FW; Trincadeira: 30.59 ± 4.59 nmol MDA g^{-1} FW). Our results are in accordance to the studies of Tománková et al. [53] that reported the detection of increased MDA content sooner in the resistant (24 hpi) that in the susceptible genotype (48 hpi) in the interaction between tomato and the powdery mildew [53]. Also, after inoculation an MLP-like protein 423 was more accumulated in Regent (6 hpi: spot 2181; 24 hpi: spots 852, 856). The major latex proteins are members of the Bet v 1 protein superfamily [54] and present a hydrophobic fold presumed to have a role in binding and translocation of hydrophobic compounds, such as flavonoids and fatty acids [55,56]. It was recently pointed out that these proteins may play a role not just in transmembrane lipid transport but also in long-

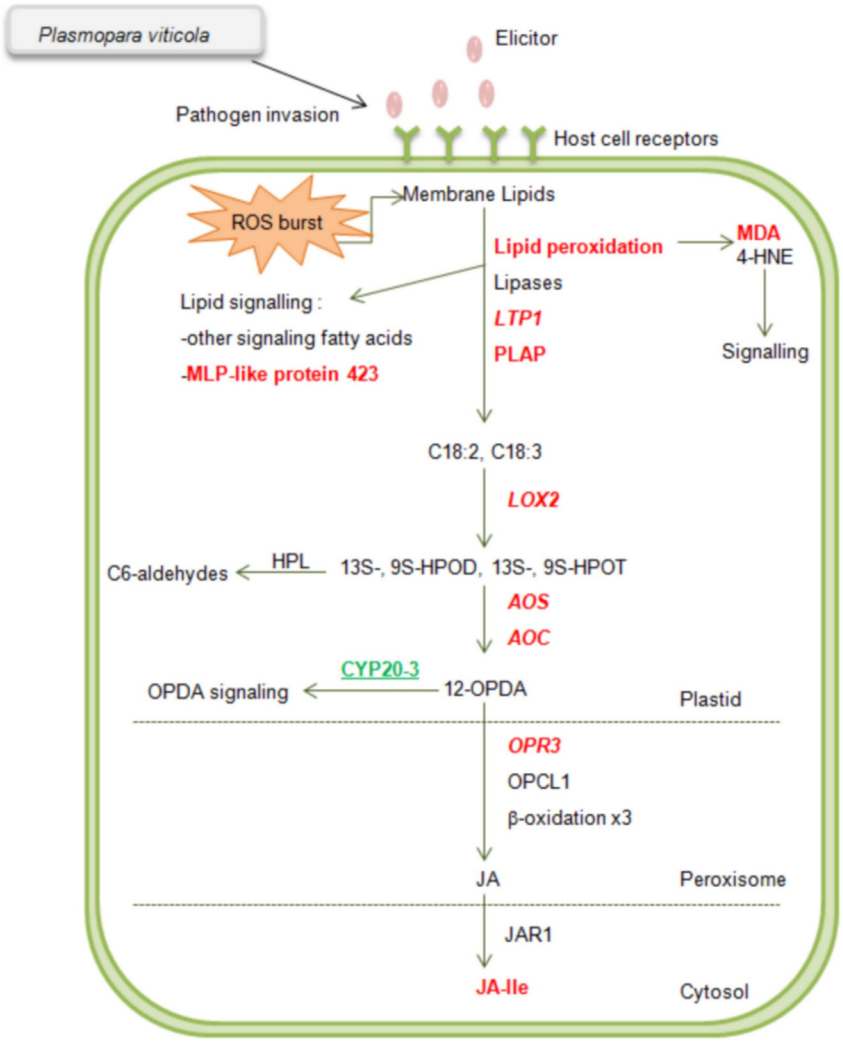

Fig. 4. Overview of the pathways involved in generation of fatty acid-derived signals. Up-regulated genes, accumulated proteins and metabolites in *V. vinifera* cv Regent are represented in red, down-accumulated proteins are represented in green. 18:1, oleic acid; 18:2, linoleic acid; 18:3, linolenic acid; MDA, Malonaldehyde; 4-HNE, 4-hydroxynonenal; LTP1- Lipid transfer protein 1; PLAP, Plastid lipid associated protein; 9S–HPODE and 13S-HPODE, 9S–hydroperoxylinoleic and 13S-hydroperoxylinoleic acid; 9S-HPOTE or 13S-HPOTE, 9S-hydroperoxylinolenic or 13S-hydroperoxylinolenic acid; HPL-hydroperoxide lyase; AOS, allene oxide synthase; AOC, allene oxide cyclase; 12-OPDA, 12-oxophytodienoic acid; OPCL1, OPC-8:0 CoA Ligase1; JAR1, Jasmonate Resistant 1; CYP20-3, peptidyl-prolyl cis-trans isomerase; MLP-like protein 423, Major Latex Like protein 423.

distance lipid transport and signalling [56]. Other evidence concerning lipid-associated signalling in this pathosystem came from our previous work [14] were a non-specific lipid transfer protein (nsLTP) presenting high homology with *V. pseudoreticulata* VpLTP1 was identified. By analyzing the expression profile during inoculation time-course it is clear that LTP1 is more expressed in Regent (6 hpi: 3.51 ± 0.34, 12 hpi: 2.26 ± 1.00, 1.94 ± 0.75, Fig. 3) than in Trincadeira. It has been recently described that nsLTP participate in plant defence mechanisms, particularly LTP1 that may be involved in long distance signalling associated with systemic acquired resistance (SAR) through interaction with lipid-derived molecules such as JA [57,58]. Moreover, at 12 hpi a plastid lipid associated protein (spot 722) presented higher levels in Regent. These proteins, also termed fibrillins, serve as scaffolds for building lipid droplets that contain free fatty acids, carotenoids, phytols, quinones, and other lipophilic compounds, some of which may be damaged as a consequence of photooxidative conditions [59]. Also, very recently it was shown a correlation between the levels of fibrillin and the production of jasmonic acid (JA) [60] in stressed plants. These authors have shown that plastoglobules may function as a specialized platform for the synthesis of early JA precursors, storing enough fatty acids (with a prevalence of C18:3) to switch on the synthesis rapidly after local oxidative stress endangering thylakoids and photosynthetic machineries [60]. Indeed, the fatty acid C18:3 presents a higher accumulation in Regent after *P. viticola* inoculation (data not show) and the expression of key genes of JA synthesis (Figs. 3 and 4) are increased in Regent when compared to Trincadeira in the first hours of interaction (*LOX2*- 12 hpi: 6.77 ± 1.71; *AOC*- 12 hpi: 3.42 ± 0.72, 24 hpi: 2.83 ± 0.015; *AOS*- 6 hpi:7.14 ± 1.69, 12 hpi: 4.57 ± 1.44 and *OPR3*- 24 hpi: 2.36 ± 0.28; Fig. 3). Both JA and its precursor 12-oxophytodienoic acid (OPDA) may mediate responses to environmental stresses. We have previously suggested a role for jasmonates in establishing or maintaining *V. vinifera* cv Regent resistance against *P. viticola*, as the expression of JA synthesis and signalling associated genes increased and JA and JA-Ile levels increased at 6 and 12 hpi [43,61]. Recently, a cyclophilin 20–3 was identified as a key effector protein that links OPDA signalling to amino acid biosynthesis and cellular redox homeostasis in stress responses [62]. The authors have show that binding of CYP20-3 to 12-OPDA promotes formation of a complex responsible for increased levels of thiol metabolites, buildup of cellular reduction potential and expression of OPDA responsive genes. During inoculation time-course a CYP20–3 protein showed low accumulation in Regent. Our results indicate that JA and not OPDA is the signalling molecule that induces the resistance response in Regent, corroborating our previous hypothesis that JA-signalling may play an important role in the establishment of Regent's resistance response (Fig. 4).

4. Concluding remarks

Several studies have been conducted on the leaf proteome modulation of susceptible grapevine cultivars after *P. viticola* inoculation. Up to our knowledge no studies have been carried on the proteome modulation neither on incompatible interactions nor in the characterization of genotype-specific adjustments of the leaf proteome after *P. viticola* inoculation. As far as we know, this is the first study that provides information about the distinct proteome changes leading to the discrimination of resistant and susceptible grapevine cultivars prior and after inoculation with the downy mildew pathogen. With a 2D–DIGE approach we were able to discriminate the two grapevine genotypes highlighting the involvement of ROS-signalling events to restrain fungal growth. Lipid associated signalling, with the involvement of jasmonic acid, also allowed cultivar discrimination, playing a major role in the establishment of the defence mechanism of the resistant cultivar. More studies have to be conducted in order to fully understand the role of lipid associated signalling in this pathosystem.

Supplementary data to this article can be found online at doi:10.1016/j.jprot.2016.10.012.

Conflict of interest

The authors declare that they have no conflict of interest.

Acknowledgments

The authors wish to acknowledge Dr. Eva Zyprian and Dr. Martina Bonow-Rex from JKI, Institute for Grapevine Breeding, Geilweilerhof for all the help provided in grapevine inoculation experiments and Dr. Andrea Lorentzen from the Department of Biochemistry and Molecular Biology of the University of Southern Denmark, for all the help provided with protein identification. This work was supported by Fundação para a Ciência e Tecnologia (FCT/MCTES/PIDDAC, Portugal) with the project PTDC/AGR-GPL/119753/2010, PEst-OE/BIA/UI 4046/2014 and grants SFRH/BPD/63641/2009 and SFRH/BPD/99712/2014.

References

[1] A. Millardet, Notes sur les vignes américaines et opuscules divers sur le même sujet, Bordeaux, 1881.
[2] P. Galet, Mildiou, Lavoisier, Paris, 1977.
[3] C. Gessler, I. Pertot, M. Perazzolli, *Plasmopara viticola*: a review of knowledge on downy mildew of grapevine and effective disease management, Phytopathol. Mediterr. 50 (1) (2011) 3–44.
[4] W. Chen, F. Delmotte, S. Richard-Cervera, L. Douence, C. Greif, M. Corio-Costet, At least two origins of fungicide resistance in grapevine downy mildew populations, Appl. Environ. Microbiol. 73 (16) (2007) 5162–5172.
[5] M. Blum, M. Waldner, U. Gisi, A single point mutation in the novel PvCesA3 gene confers resistance to the carboxylic acid amide fungicide mandipropamid in *Plasmopara viticola*, Fungal Genet. Biol. 47 (6) (2010) 499–510.
[6] E. Peressotti, S. Wiedemann-Merdinoglu, F. Delmotte, D. Bellin, G. Di Gaspero, R. Testolin, D. Merdinoglu, P. Mestre, Breakdown of Resistance to Grapevine Downy Mildew upon Limited Deployment of a Resistant Variety, Bmc Plant Biology 10, 2010.
[7] K. Casagrande, L. Falginella, S. Castellarin, R. Testolin, G. Di Gaspero, Defence responses in Rpv3-dependent resistance to grapevine downy mildew, Planta 234 (6) (2011) 1097–1109.
[8] M. Polesani, L. Bortesi, A. Ferrarini, A. Zamboni, M. Fasoli, C. Zadra, A. Lovato, M. Pezzotti, M. Delledonne, A. Polverari, General and species-specific transcriptional responses to downy mildew infection in a susceptible (*Vitis vinifera*) and a resistant (*V. riparia*) grapevine species, BMC Genomics 11 (2010).
[9] A. Diez-Navajas, S. Wiedemann-Merdinoglu, C. Greif, D. Merdinoglu, Nonhost versus host resistance to the grapevine downy mildew, *Plasmopara viticola*, studied at the tissue level, Phytopathology 98 (7) (2008) 776–780.
[10] G. Di Gaspero, G. Cipriani, A. Adam-Blondon, R. Testolin, Linkage maps of grapevine displaying the chromosomal locations of 420 microsatellite markers and 82 markers for R-gene candidates, Theor. Appl. Genet. 114 (7) (2007) 1249–1263.
[11] M. Hamiduzzaman, G. Jakab, L. Barnavon, J. Neuhaus, B. Mauch-Mani, beta-Aminobutyric acid-induced resistance against downy mildew in grapevine acts through the potentiation of callose formation and jasmonic acid signaling, Mol. Plant-Microbe Interact. 18 (8) (2005) 819–829.
[12] A. Kortekamp, Expression analysis of defence-related genes in grapevine leaves after inoculation with a host and a non-host pathogen, Plant Physiol. Biochem. 44 (1) (2006) 58–67.
[13] S. Trouvelot, A. Varnier, M. Allegre, L. Mercier, F. Baillieul, C. Arnould, V. Gianinazzi-Pearson, O. Klarzynski, J. Joubert, A. Pugin, X. Daire, A beta-1,3 glucan sulfate induces resistance in grapevine against *Plasmopara viticola* through priming of defense responses, including HR-like cell death, Mol. Plant-Microbe Interact. 21 (2) (2008) 232–243.
[14] A. Figueiredo, F. Monteiro, A. Fortes, M. Bonow-Rex, E. Zyprian, L. Sousa, M. Pais, Cultivar-specific kinetics of gene induction during downy mildew early infection in grapevine, Funct. Integr. Genomics 12 (2) (2012) 379–386.
[15] A. Milli, D. Cecconi, L. Bortesi, A. Persi, S. Rinalducci, A. Zamboni, G. Zoccatelli, A. Lovato, L. Zolla, A. Polverari, Proteomic analysis of the compatible interaction between *Vitis vinifera* and *Plasmopara viticola*, J. Proteome 75 (4) (2012) 1284–1302.
[16] A. Figueiredo, A. Fortes, S. Ferreira, M. Sebastiana, Y. Choi, L. Sousa, B. Acioli-Santos, F. Pessoa, R. Verpoorte, M. Pais, Transcriptional and metabolic profiling of grape (*Vitis vinifera* L.) leaves unravel possible innate resistance against pathogenic fungi, J. Exp. Bot. 59 (12) (2008) 3371–3381.
[17] K. Ali, F. Maltese, A. Figueiredo, M. Rex, A. Fortes, E. Zyprian, M. Pais, R. Verpoorte, Y. Choi, Alterations in grapevine leaf metabolism upon inoculation with *Plasmopara viticola* in different time-points, Plant Sci. 191 (2012) 100–107.
[18] M. Giribaldi, M. Giuffrida, Heard it through the grapevine: proteomic perspective on grape and wine, J. Proteome 73 (9) (2010) 1647–1655.
[19] M. Palmieri, M. Perazzolli, V. Matafora, M. Moretto, A. Bachi, I. Pertot, Proteomic analysis of grapevine resistance induced by Trichoderma harzianum T39 reveals specific defence pathways activated against downy mildew, J. Exp. Bot. 63 (17) (2012) 6237–6251.
[20] A. Kortekamp, L. Welter, S. Vogt, A. Knoll, F. Schwander, R. Topfer, E. Zyprian, Identification, isolation and characterization of a CC-NBS-LRR candidate disease resistance gene family in grapevine, Mol. Breed. 22 (3) (2008) 421–432.

[21] M. Sebastiana, A. Figueiredo, F. Monteiro, J. Martins, C. Franco, A.V. Coelho, F. Vaz, T. Simões, D. Penque, M.S. Pais, S. Ferreira, A possible approach for gel-based proteomic studies in recalcitrant woody plants, Springerplus 2 (1) (2013) 1–16.
[22] V. Neuhoff, N. Arold, D. Taube, W. Ehrhardt, Improved staining of proteins in polyacrylamide gels including isoelectric, Electrophoresis 9 (6) (1988) 255–262.
[23] G. da Costa, E. Lamy, F.C.e. Silva, J. Andersen, E.S. Baptista, A.V. Coelho, Salivary amylase induction by tannin-enriched diets as a possible countermeasure against tannins, J. Chem. Ecol. 34 (3) (2008) 376–387.
[24] R. Velasco, A. Zharkikh, M. Troggio, D. Cartwright, A. Cestaro, D. Pruss, M. Pindo, L. FitzGerald, S. Vezzulli, J. Reid, G. Malacarne, D. Iliev, G. Coppola, B. Wardell, D. Micheletti, T. Macalma, M. Facci, J. Mitchell, M. Perazzolli, G. Eldredge, P. Gatto, R. Oyzerski, M. Moretto, N. Gutin, M. Stefanini, Y. Chen, C. Segala, C. Davenport, L. Dematte, A. Mraz, J. Battilana, K. Stormo, F. Costa, Q. Tao, A. Si-Ammour, T. Harkins, A. Lackey, C. Perbost, B. Taillon, A. Stella, V. Solovyev, J. Fawcett, L. Sterck, K. Vandepoele, S. Grando, S. Toppo, C. Moser, J. Lanchbury, R. Bogden, M. Skolnick, V. Sgaramella, S. Bhatnagar, P. Fontana, A. Gutin, Y. Van de Peer, F. Salamini, R. Viola, A high quality draft consensus sequence of the genome of a heterozygous grapevine variety, PLoS One 2 (12) (2007).
[25] J. Vizcaino, E. Deutsch, R. Wang, A. Csordas, F. Reisinger, D. Rios, J. Dianes, Z. Sun, T. Farrah, N. Bandeira, P. Binz, I. Xenarios, M. Eisenacher, G. Mayer, L. Gatto, A. Campos, R. Chalkley, H. Kraus, J. Albar, S. Martinez-Bartolome, R. Apweiler, G. Omenn, L. Martens, A. Jones, H. Hermjakob, ProteomeXchange provides globally coordinated proteomics data submission and dissemination, Nat. Biotechnol. 32 (3) (2014) 223–226.
[26] A. Conesa, S. Gotz, J. Garcia-Gomez, J. Terol, M. Talon, M. Robles, Blast2GO: a universal tool for annotation, visualization and analysis in functional genomics research, Bioinformatics 21 (18) (2005) 3674–3676.
[27] R. CHILDS, W. BARDSLEY, Steady-state kinetics of peroxidase with 2,2′-azino-di-(3-ethylbenzthiazoline-6-sulphonic acid) as chromogen, Biochem. J. 145 (1) (1975) 93–103.
[28] D. Hodges, J. DeLong, C. Forney, R. Prange, Improving the thiobarbituric acid-reactive-substances assay for estimating lipid peroxidation in plant tissues containing anthocyanin and other interfering compounds, Planta 207 (4) (1999) 604–611.
[29] J. Hellemans, G. Mortier, A. De Paepe, F. Speleman, J. Vandesompele, qBase relative quantification framework and software for management and automated analysis of real-time quantitative PCR data, Genome Biol. 8 (2) (2007).
[30] M. Khan, I. Khan, H. Ahmad, H. Ali, S. Ghafoor, M. Afzal, F. Khan, M. Shah, S. Afridi, Estimation of genetic diversity in walnut, Pak. J. Bot. 42 (3) (2010) 1791–1796.
[31] J. Xu, L. Pascual, R. Aurand, J. Bouchet, B. Valot, M. Zivy, M. Causse, M. Faurobert, An extensive proteome map of tomato (*Solanum lycopersicum*) fruit pericarp, Proteomics 13 (20) (2013) 3059–3063.
[32] S. Kundu, D. Chakraborty, A. Kundu, A. Pal, Proteomics Approach Combined with Biochemical Attributes to Elucidate Compatible and Incompatible Plant-Virus Interactions Between *Vigna mungo* and Mungbean Yellow Mosaic India Virus, Proteome Science 11, 2013.
[33] H. Moura, I. Vasconcelos, C. Souza, F. Silva, F. Moreno, M. Lobo, A. Monteiro-Moreira, A. Moura, J. Costa, J. Oliveira, Proteomics changes during the incompatible interaction between cowpea and *Colletotrichum gloeosporioides* (Penz.) Penz and Sacc, Plant Sci. 217 (2014) 158–175.
[34] M. Torres, J. Jones, J. Dangl, Reactive oxygen species signaling in response to pathogens, Plant Physiol. 141 (2) (2006) 373–378.
[35] R. Mittler, S. Vanderauwera, M. Gollery, F. Van Breusegem, Reactive oxygen gene network of plants, Trends Plant Sci. 9 (10) (2004) 490–498.
[36] X. Chen, X. Wang, Z. Zhang, Y. Wang, X. Zheng, Differences in the induction of the oxidative burst in compatible and incompatible interactions of soybean and *Phytophthora sojae*, Physiol. Mol. Plant Pathol. 73 (1–3) (2008) 16–24.
[37] S. Mandal, R. Das, S. Mishra, Differential occurrence of oxidative burst and antioxidative mechanism in compatible and incompatible interactions of *Solanum lycopersicum* and *Ralstonia solanacearum*, Plant Physiol. Biochem. 49 (2) (2011) 117–123.
[38] C. Foyer, G. Noctor, Redox homeostasis and antioxidant signaling: a metabolic interface between stress perception and physiological responses, Plant Cell 17 (7) (2005) 1866–1875.
[39] R. Mittler, E. Herr, B. Orvar, W. van Camp, H. Willekens, D. Inze, B. Ellis, Transgenic tobacco plants with reduced capability to detoxify reactive oxygen intermediates are hyperresponsive to pathogen infection, Proc. Natl. Acad. Sci. U. S. A. 96 (24) (1999) 14165–14170.
[40] D. Klessig, J. Durner, R. Noad, D. Navarre, D. Wendehenne, D. Kumar, J. Zhou, J. Shah, S. Zhang, P. Kachroo, Y. Trifa, D. Pontier, E. Lam, H. Silva, Nitric oxide and salicylic acid signaling in plant defense, Proc. Natl. Acad. Sci. U. S. A. 97 (16) (2000).
[41] G. Pastori, G. Kiddle, J. Antoniw, S. Bernard, S. Veljovic-Jovanovic, P. Verrier, G. Noctor, C. Foyer, Leaf vitamin C contents modulate plant defense transcripts and regulate genes that control development through hormone signaling, Plant Cell 15 (4) (2003) 939–951.
[42] C. Barth, W. Moeder, D. Klessig, P. Conklin, The timing of senescence and response to pathogens is altered in the ascorbate-deficient Arabidopsis mutant vitamin c-1, Plant Physiol. 134 (4) (2004) 1784–1792.
[43] A. Guerreiro, J. Figueiredo, M. Sousa Silva, A. Figueiredo, Linking jasmonic acid to grapevine resistance against the biotrophic oomycete *Plasmopara viticola*, Front. Plant Sci. (2016).
[44] A. Herrera-Vasquez, P. Salinas, L. Holuigue, Salicylic acid and reactive oxygen species interplay in the transcriptional control of defense genes expression, Front. Plant Sci. 6 (2015).
[45] M. Romero-Puertas, M. Laxa, A. Matte, F. Zaninotto, I. Finkemeier, A. Jones, M. Perazzolli, E. Vandelle, K. Dietz, M. Delledonne, S-nitrosylation of peroxiredoxin II E promotes peroxynitrite-mediated tyrosine nitration, Plant Cell 19 (12) (2007) 4120–4130.
[46] S. Lee, D. Lee, Y. Lee, U. Mayer, Y. Stierhof, G. Jurgens, I. Hwang, Heat shock protein cognate 70-4 and an E3 ubiquitin ligase, CHIP, mediate plastid-destined precursor degradation through the ubiquitin-26S proteasome system in Arabidopsis, Plant Cell 21 (12) (2009) 3984–4001.
[47] L. Noel, G. Cagna, J. Stuttmann, L. Wirthmuller, S. Betsuyaku, C. Witte, R. Bhat, N. Pochon, T. Colby, J. Parker, Interaction between SGT1 and Cytosolic/Nuclear HSC70 chaperones regulates Arabidopsis immune responses, Plant Cell 19 (12) (2007) 4061–4076.
[48] Y. Qi, H. Wang, Y. Zou, C. Liu, Y. Liu, Y. Wang, W. Zhang, Over-expression of mitochondrial heat shock protein 70 suppresses programmed cell death in rice, FEBS Lett. 585 (1) (2011) 231–239.
[49] N. Kim, B. Hwang, Pepper heat shock protein 70a interacts with the type III effector AvrBsT and triggers plant cell death and immunity, Plant Physiol. 167 (2) (2015) 307–U499.
[50] D. Baek, Y. Jin, J. Jeong, H. Lee, H. Moon, J. Lee, D. Shin, C. Kang, D. Kim, J. Nam, S. Lee, D. Yun, Suppression of reactive oxygen species by glyceraldehyde-3-phosphate dehydrogenase, Phytochemistry 69 (2) (2008) 333–338.
[51] J. Walley, D. Kliebenstein, R. Bostock, K. Dehesh, Fatty acids and early detection of pathogens, Curr. Opin. Plant Biol. 16 (4) (2013) 520–526.
[52] A. Ayala, M. Munoz, S. Arguelles, Lipid peroxidation: production, metabolism, and signaling mechanisms of malondialdehyde and 4-hydroxy-2-nonenal, Oxidative Med. Cell. Longev. (2014).
[53] K. Tomankova, L. Luhova, M. Petrivalsky, P. Pec, A. Lebeda, Biochemical aspects of reactive oxygen species formation in the interaction between *Lycopersicon* spp. and *Oidium neolycopersici*, Physiol. Mol. Plant Pathol. 68 (1–3) (2006) 22–32.
[54] C. Radauer, H. Breiteneder, Classification of allergen-containing protein families into structural superfamilies reveals that most structural homologues of allergens are non-allergenic, Allergy 63 (2008) 570.
[55] J. Chen, X. Dai, Cloning and characterization of the *Gossypium hirsutum* major latex protein gene and functional analysis in *Arabidopsis thaliana*, Planta 231 (4) (2010) 861–873.
[56] B. Guelette, U. Benning, S. Hoffmann-Benning, Identification of lipids and lipid-binding proteins in phloem exudates from *Arabidopsis thaliana*, J. Exp. Bot. 63 (10) (2012) 3603–3616.
[57] T. Girault, J. Francois, H. Rogniaux, S. Pascal, S. Delrot, P. Coutos-Thevenot, E. Gomes, Exogenous application of a lipid transfer protein-jasmonic acid complex induces protection of grapevine towards infection by *Botrytis cinerea*, Plant Physiol. Biochem. 46 (2) (2008) 140–149.
[58] F. Liu, X. Zhang, C. Lu, X. Zeng, Y. Li, D. Fu, G. Wu, Non-specific lipid transfer proteins in plants: presenting new advances and an integrated functional analysis, J. Exp. Bot. 66 (19) (2015) 5663–5681.
[59] C. Brehelin, F. Kessler, K. van Wijk, Plastoglobules: versatile lipoprotein particles in plastids, Trends Plant Sci. 12 (6) (2007) 260–266.
[60] A. Youssef, Y. Laizet, M. Block, E. Marechal, J. Alcaraz, T. Larson, D. Pontier, J. Gaffe, M. Kuntz, Plant lipid-associated fibrillin proteins condition jasmonate production under photosynthetic stress, Plant J. 61 (3) (2010) 436–445.
[61] A. Figueiredo, F. Monteiro, M. Sebastiana, First clues on a jasmonic acid role in grapevine resistance against the biotrophic fungus *Plasmopara viticola*, Eur. J. Plant Pathol. 142 (3) (2015) 645–652.
[62] S. Park, W. Li, A. Viehhauser, B. He, S. Kim, A. Nilsson, M. Andersson, J. Kittle, M. Ambavaram, S. Luan, A. Esker, D. Tholl, D. Cimini, M. Ellerstrom, G. Coaker, T. Mitchell, A. Pereira, K. Dietz, C. Lawrence, Cyclophilin 20-3 relays a 12-oxo-phytodienoic acid signal during stress responsive regulation of cellular redox homeostasis, Proc. Natl. Acad. Sci. U. S. A. 110 (23) (2013) 9559–9564.